ARPES on High Temperature Superconductors: Benefits of the Surface Sensitivity

Plan:

"Surface States" in BISCO?

ALS-CXRO seminar
July 16th, 2003

Photoemission is a surface sensitive technique

M.P. Seah & W.A. Dench,
Surf. Interface Anal. 1 (1979)

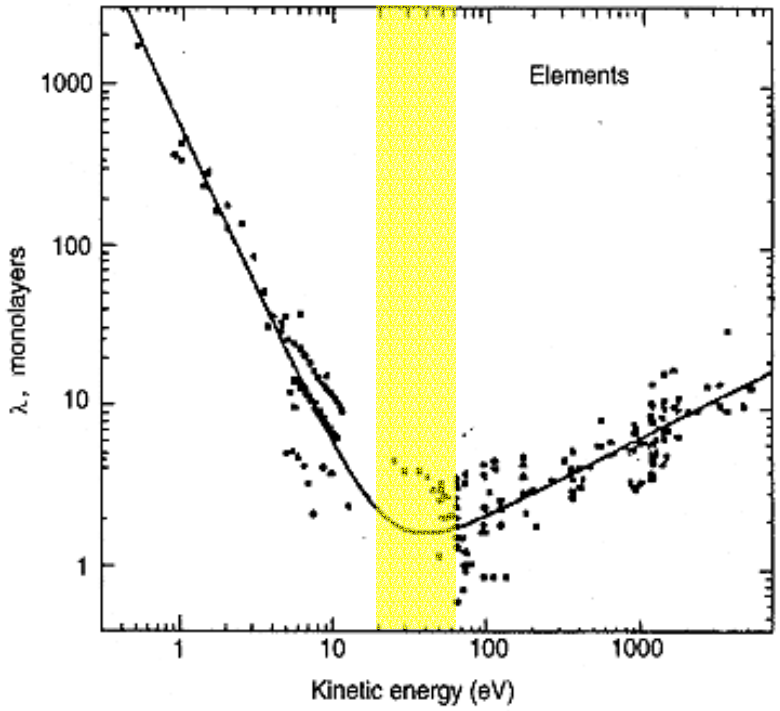

BISCO sample

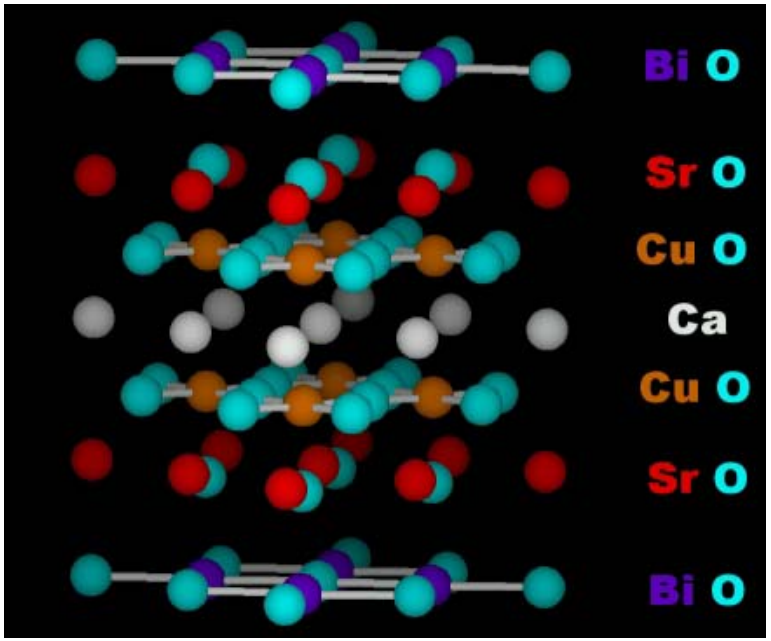

How to search for the surface states?

- They do not disperse with $k_\perp$ (doesn't help: HTSC are 2-D)
- Surface impurities usually kill them right away

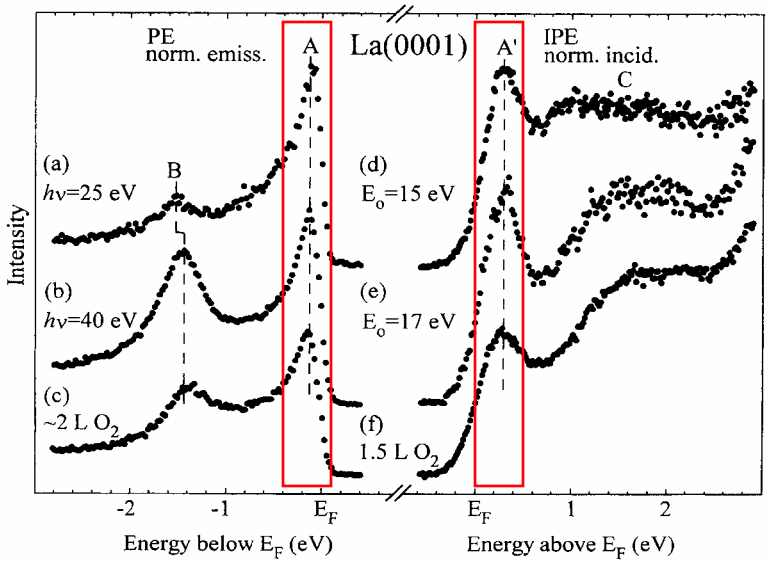

FIG. 1. Left panel: Photoemission spectra of La(0001) taken at $h\nu = 25$ eV (a) and $h\nu = 40$ eV (b) for a clean and well-ordered surface; (c) PE spectrum after adsorption of $\cong 2$ Langmuir (1 L $= 10^{-6}$ Torr s) O_2 taken at $h\nu = 40$ eV. The spectra are normalized to the same incident photon flux. Right panel: Inverse photoemission spectra taken at primary electron energy of $E_0 = 15$ eV (d) and $E_0 = 17$ eV (e) of a clean and well-ordered La(0001); (f) IPE spectrum taken at $E_0 = 17$ eV after adsorption of 1.5 L O_2.

Surface States have been found at:

$YBa_2Co_3O_{7-\delta}$: D.H. Lu et al., PRL 86, 4370 (2001)

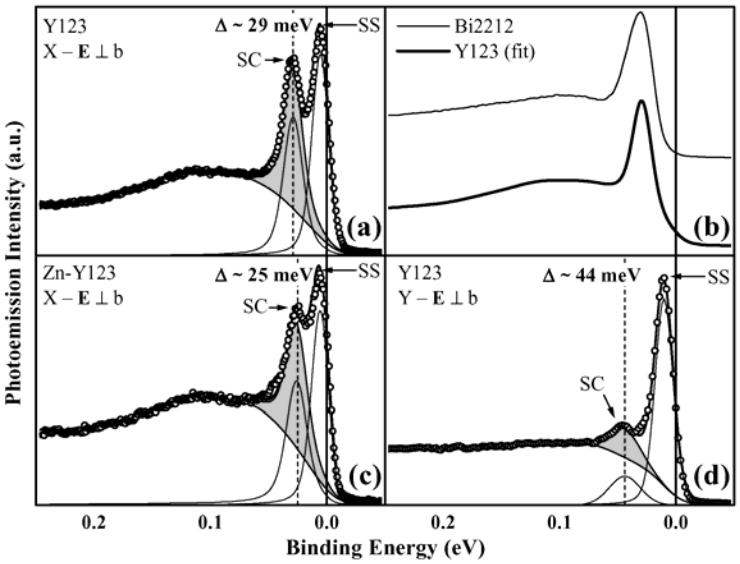

FIG. 3. (a) EDC at X reproduced from Fig. 1a together with fitting curves. Panel (b) compares the fitting curve (after subtracting the surface state peak) with the EDC from overdoped Bi2212 ($T_c = 84$ K) at $(\pi,0)$. (c) EDC at X from Zn-doped Y123 with fitting curves. (d) EDC at Y from Y123 with fitting curves. All data shown were taken at 10 K. Shaded area represents weight of the superconducting peak.

Sr_2RuO_4: A. Damascelli et al. PRL 85, 5194 (2000)

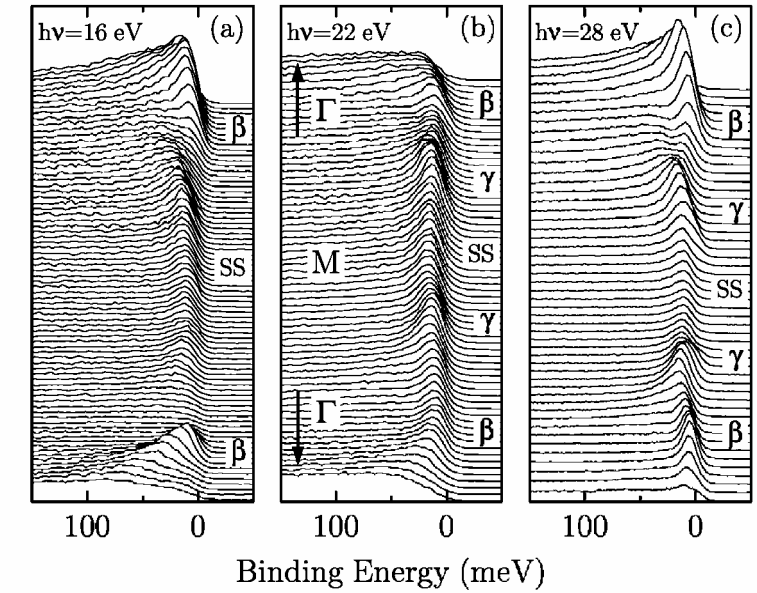

FIG. 2. ARPES spectra along Γ-M-Γ, at three different photon energies. The cuts are centered at the M point and extend beyond the γ and β FS crossings in both the first and second zones.

Photoelectron escape depth in BISCO is ~3Å

M.R. Norman et al.,
PRB 59, 11191 (1999)

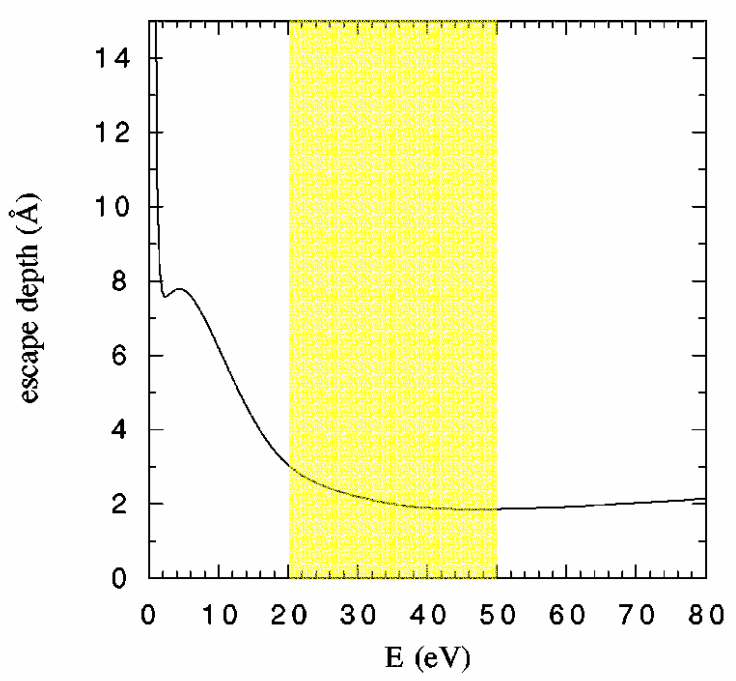

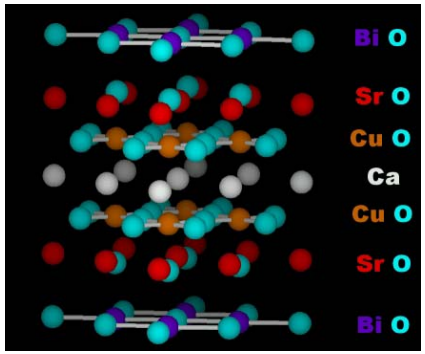

Could surface impurities help?

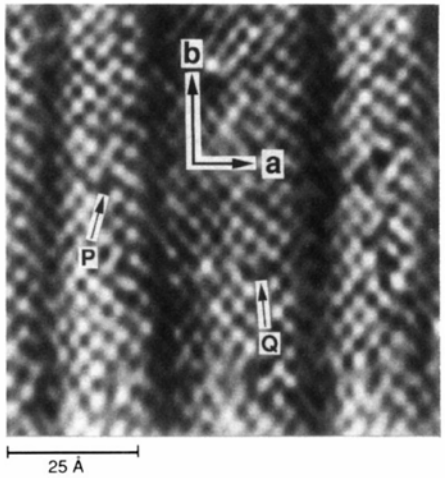

FIG. 1. 85×85 Å² STM image of cleaved $Bi_2Sr_2CaCu_2O_8$(001) acquired at tip bias of 1 V and tunneling current of 0.18 nA. The stripes parallel to the *b* axis reflect height modulations perpendicular to the *a*-*b* plane. The spacing between stripes is typically 4.5–5 tetragonal unit cells along the *a* axis. The central portion of Fig. 1 shows an unusually large modulation period. Point defects are common on the surface, as marked by *P* and *Q*.

Even chemically passive Ag and Au atoms proved to be deadly for the surface BiO layer of BISCO:

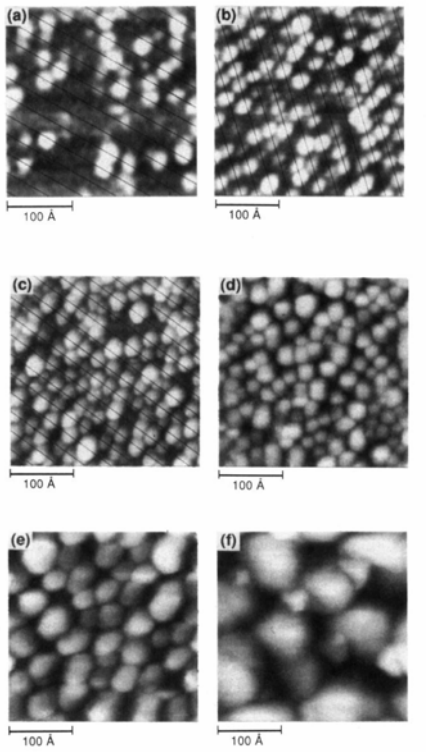

FIG. 2. (a)–(f) STM images taken after Ag depositions of 0.1, 0.2, 0.6, 1, 5, and 20 Å. The sizes of these images are 310×310 Å², except 290×290 Å² for 0.1-Å Ag deposition. Tip biases ranged from −2 to −2.34 V and tunneling currents were 0.03 to 0.5 nA. Lines parallel to the *b* axis with spacing of 25 Å are superimposed on (a)–(c) to show cluster alignment. The cluster volumes are many times the amount of Ag deposited because they reflect the conversion of planar Bi-O to Bi_2O_3-like clusters induced by Ag clustering. Ag accumulates over the Bi_2O_3 clusters after conversion of the Bi-O layer is complete, and images (d)–(f) reflect Ag aggregation.

BiO transforms into Bi_2O_3

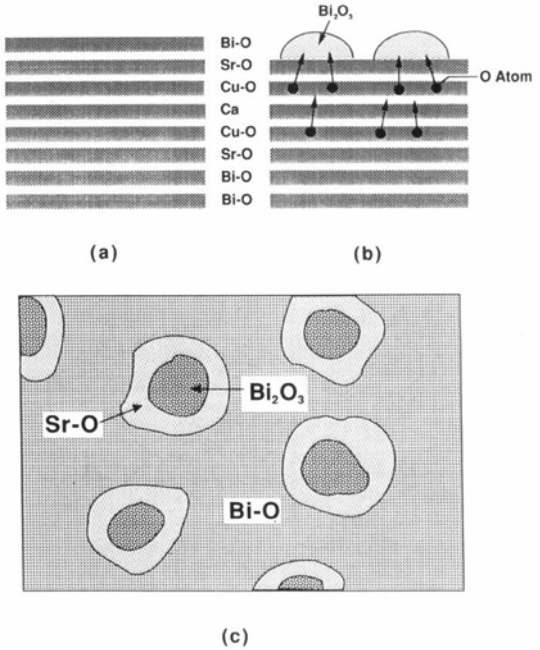

FIG. 3. (a) Schematic cross section of the $Bi_2Sr_2CaCu_2O_8$ layered structure parallel to the *c* direction before Ag deposition with a Bi-O plane terminating the structure. (b) Schematic showing conversion of the top Bi-O plane into Bi_2O_3-like species and O withdrawal from the Cu-O double layer. Ag clusters account for less than 20% of the surface and are omitted. (c) Schematic top view of the $Bi_2Sr_2CaCu_2O_8$ surface after Ag deposition depicting partial conversion of the Bi-O plane as Bi_2O_3-like clusters are formed. Structural changes involving the Bi-O plane expose the Sr-O plane around the clusters.

Y.S. Luo, Y.N. Yang, and J.H. Weaver, PRB 46, 1114 (1992)

Altering surface properties of BISCO: Few clues from the classics papers

Z.-X. Shen et al., PRL 70, 1553 (1993)

Although the qualitative trend of gap variation in **k** space is very reproducible, the gap size shows some scatter along the Γ-Y line. In Fig. 3(b), samples 1 and 3 show a very small gap along Γ-Y (where $|\cos k_x a - \cos k_y a| = 0$), while sample 2 shows a significantly larger gap in this region. A hint for the explanation of the scatter in the data can be found in the time dependence of the spectra from sample 3 taken along the Γ-Y direction and the sample quality as indicated by the laser reflection. The earliest spectrum from sample 3 was taken 1.5 h after the cleave and showed a small (1.5 meV) gap. Approximately 7 h later, the gap at that point was observed to grow to 6.5 meV, after which time it again shrank to near zero after the sample surface was regenerated. The direction of this time dependence is, interest-

H. Ding et al., PRB 1333 (1994)

2212. The signature of this *d*-wave gap are the nodes in **K**-space. The observation of a negligible gap along Γ-X and Γ-Y might be a manifestation of such nodes. On the other hand, the observation of an isotropic gap in some cleaves might indicate that impurities or defects near sample surfaces influence the gap anisotropy. Shen *et al.* have observed that, when samples are aged *in situ*, the gap tends to become more isotropic.[9] They attribute this effect to surface scattering resulting from adsorbed gases.

As recently pointed out by Norman,[14] such impurity effects, if they result from enhanced scattering, can be better explained within the framework of anisotropic *s*-wave pairing. In *d*-wave pairing, impurity scattering destroys the gap rather than rendering it isotropic, whereas in anisotropic *s*-wave pairing impurities tend to drive the gap toward its average value. However, the detailed dependence of gap anisotropy on impurities and defects in Bi-2212 remains unclear; further experiments are necessary to settle this issue.

Gap size vs. Time

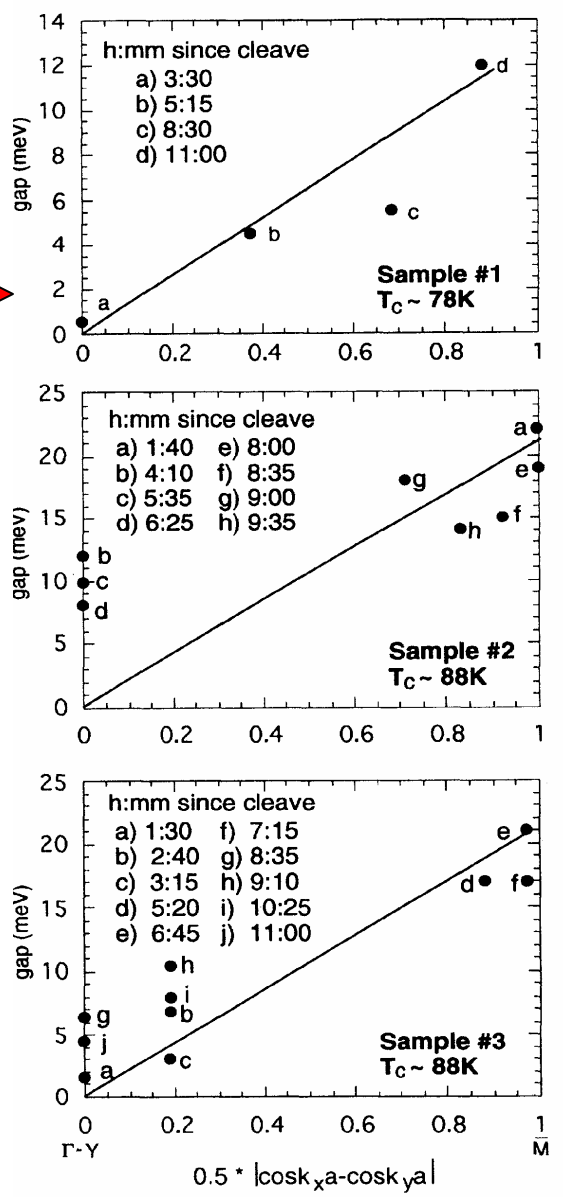

I. Vobornik et al.,
Physica C 317-318, 589 (1999)

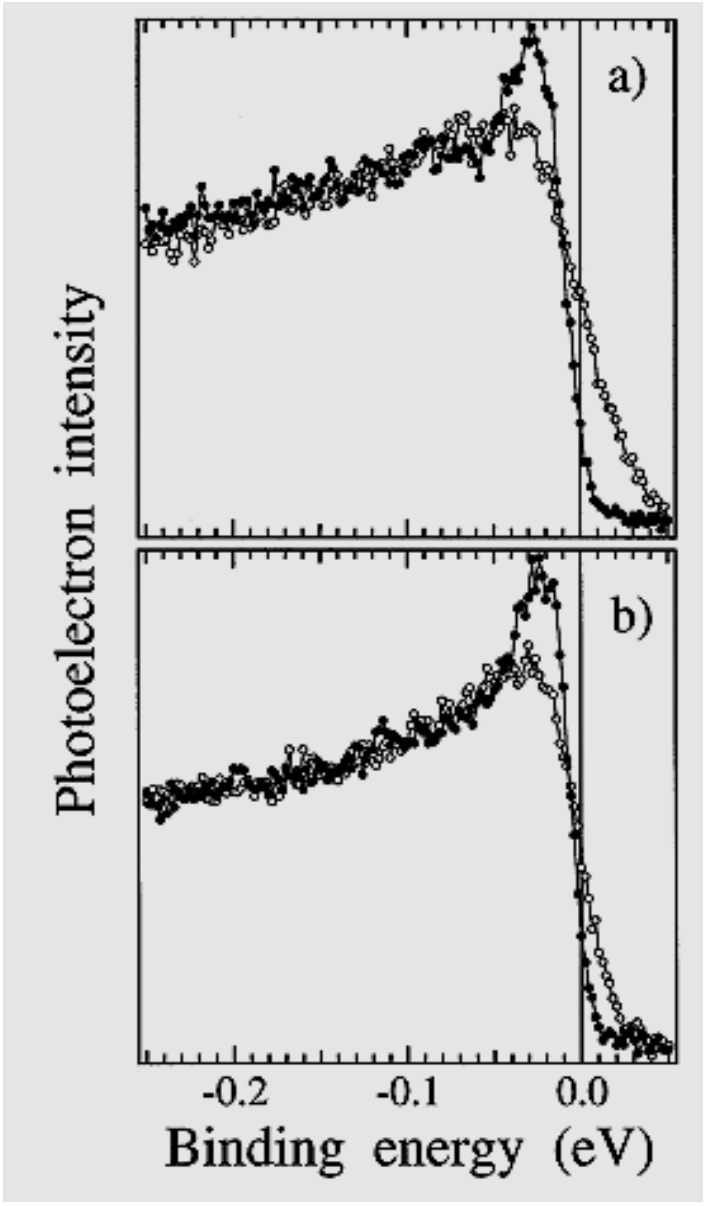

Additional clues?

Gap along the "gap node"
in over-doped BISCO

Non-zero gap along three
major directions,including
the "gap node"

R.J. Kelly et al., PRB 50, 590 (1994)

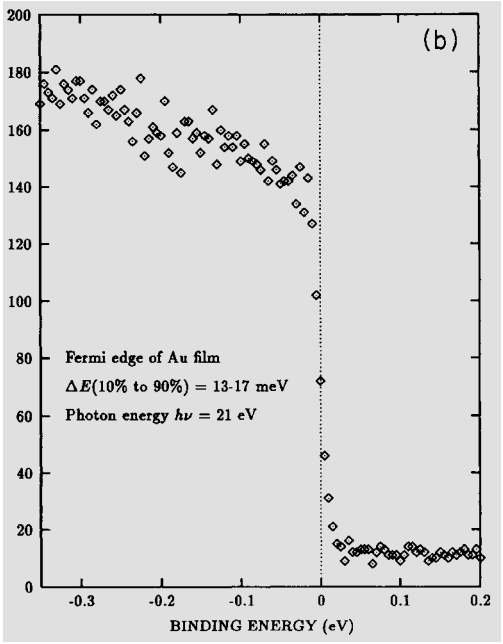

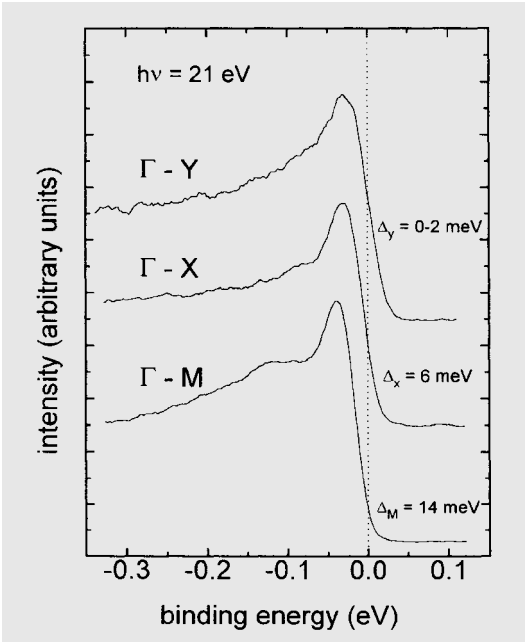

Steady look at $(\pi\text{-}\pi)$ dispersions helps to see interesting things

P.V. Bogdanov et al.,
PRL 85, 2581 (2000)

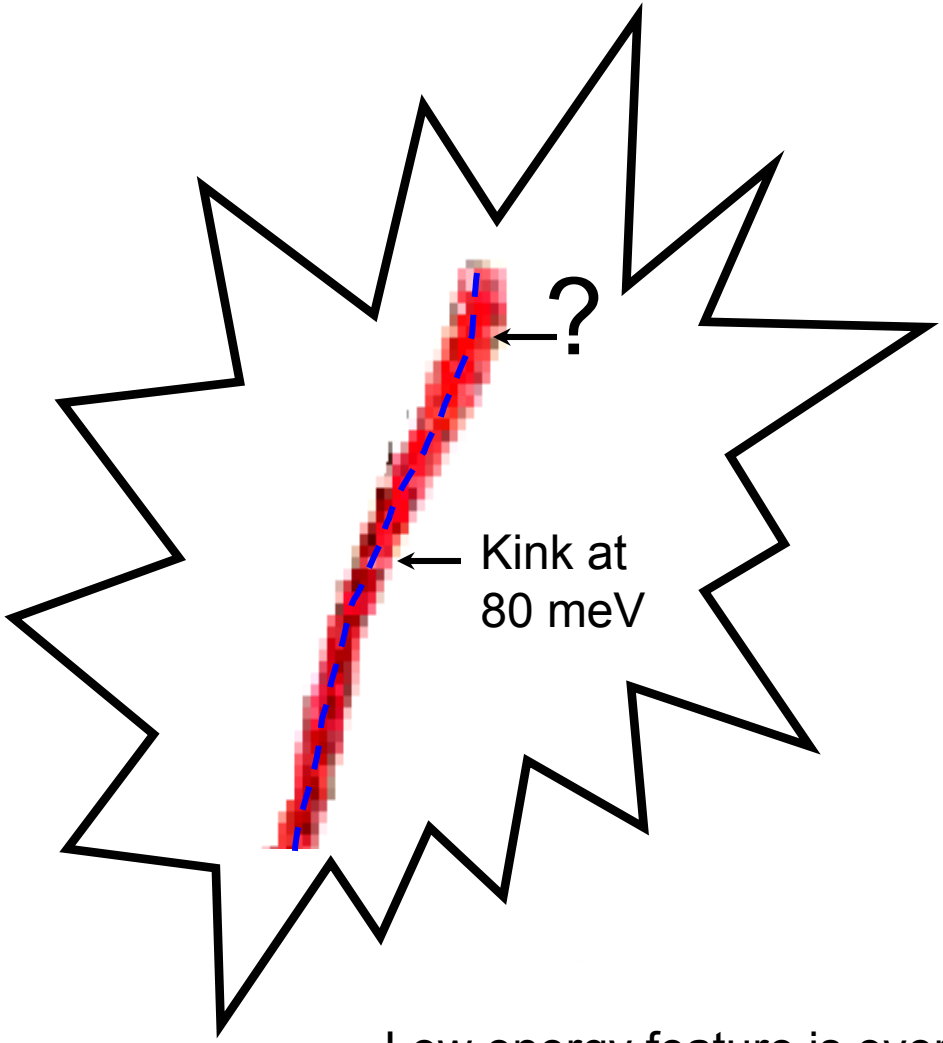

Low energy feature is everywhere $\Rightarrow$

A. Kaminski et al.,
PRL 86, 1071 (2001)

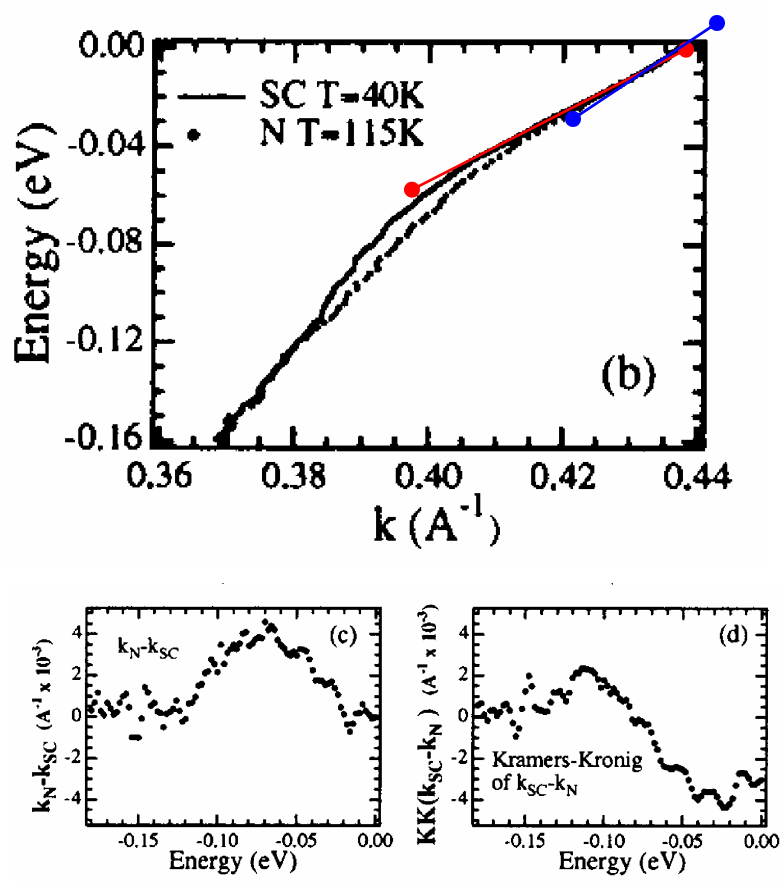

P.D. Johnson et al.,
PRL 87, 177007 (2001)

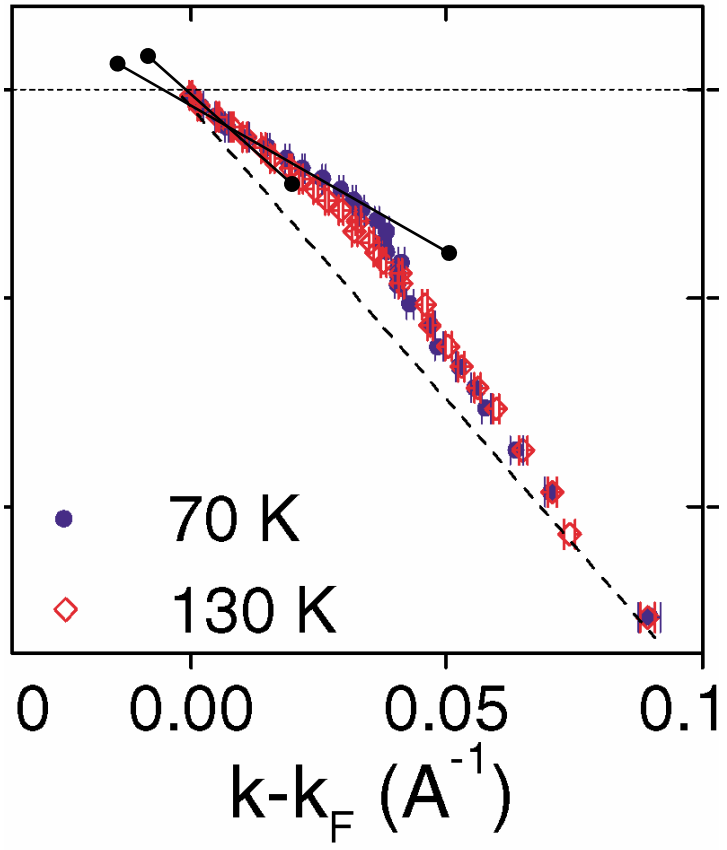

Presence of the Gap can alter dispersion derived from MDC

M.R. Norman et al.,
PRB 64, 184508 (2001)

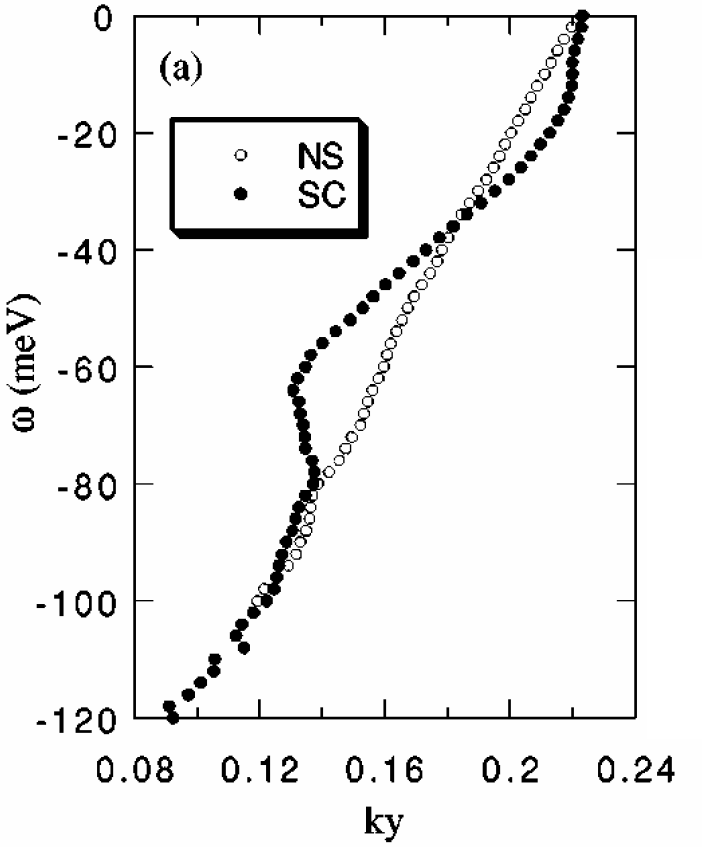

In BISCO effect is very clear at (π;0) points

A.D. Gromko et al., Cond-mat/0205329

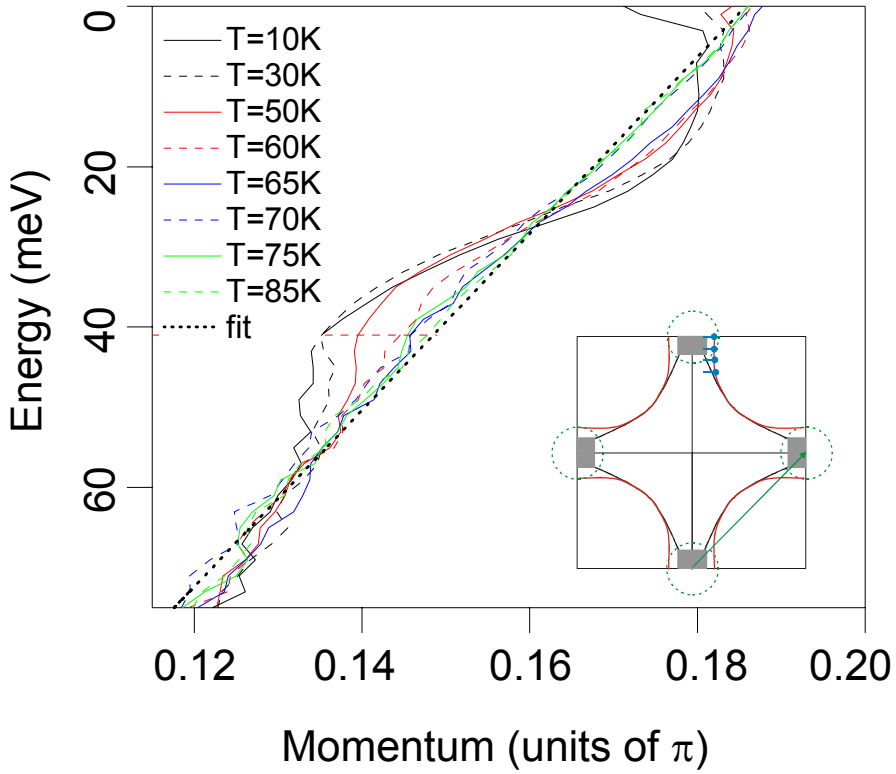

Experiment:

ARPES

Scienta SES-200

He-I radiation, 21.2 eV

ΔE=20 meV

$\leq 3 \times 10^{-11}$ Torr

Optimally doped BISCO

T_C=91 K

T=26 K

Dispersion along the “gap node” at 26 K

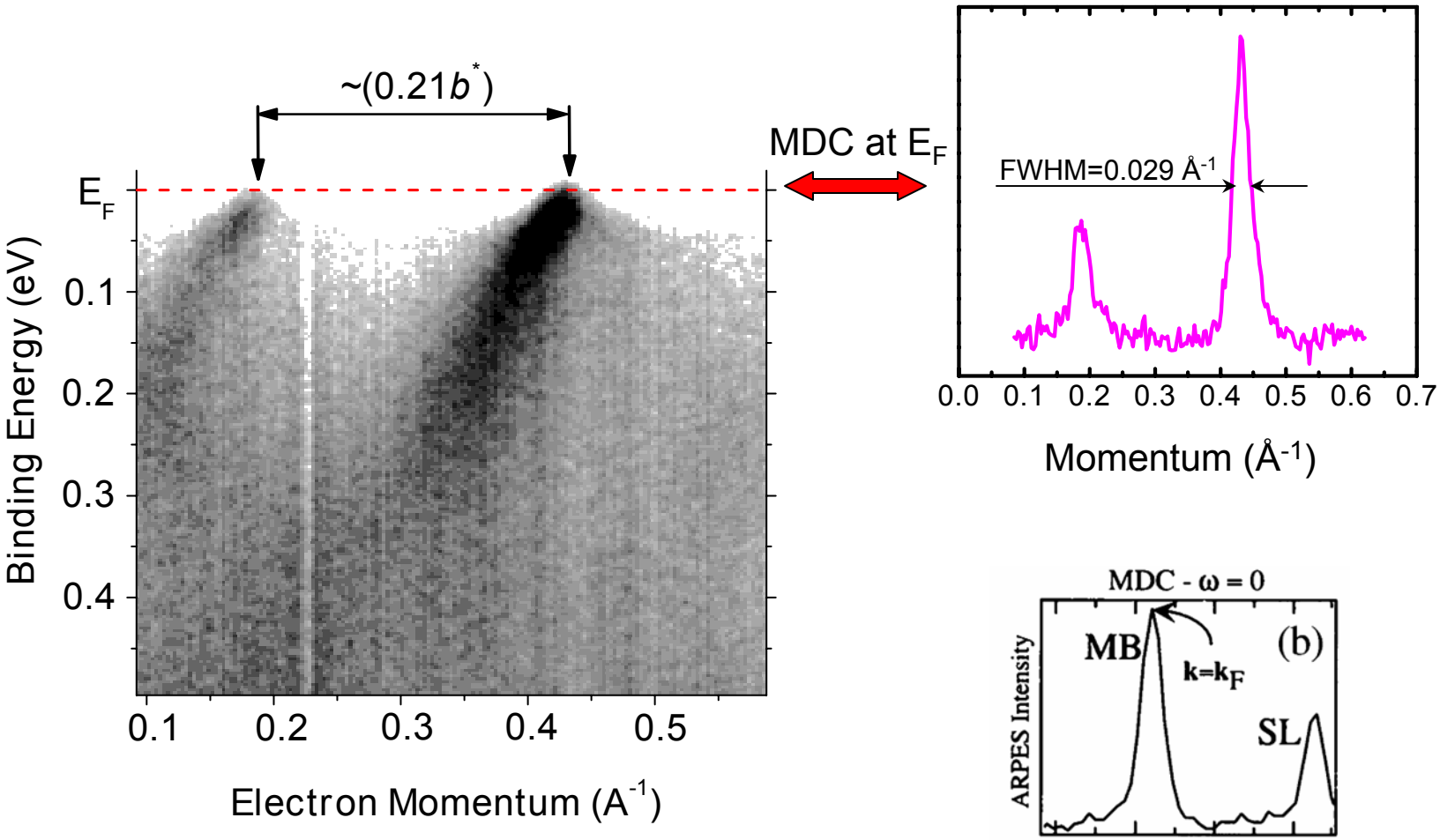

A. Kaminski et al.,

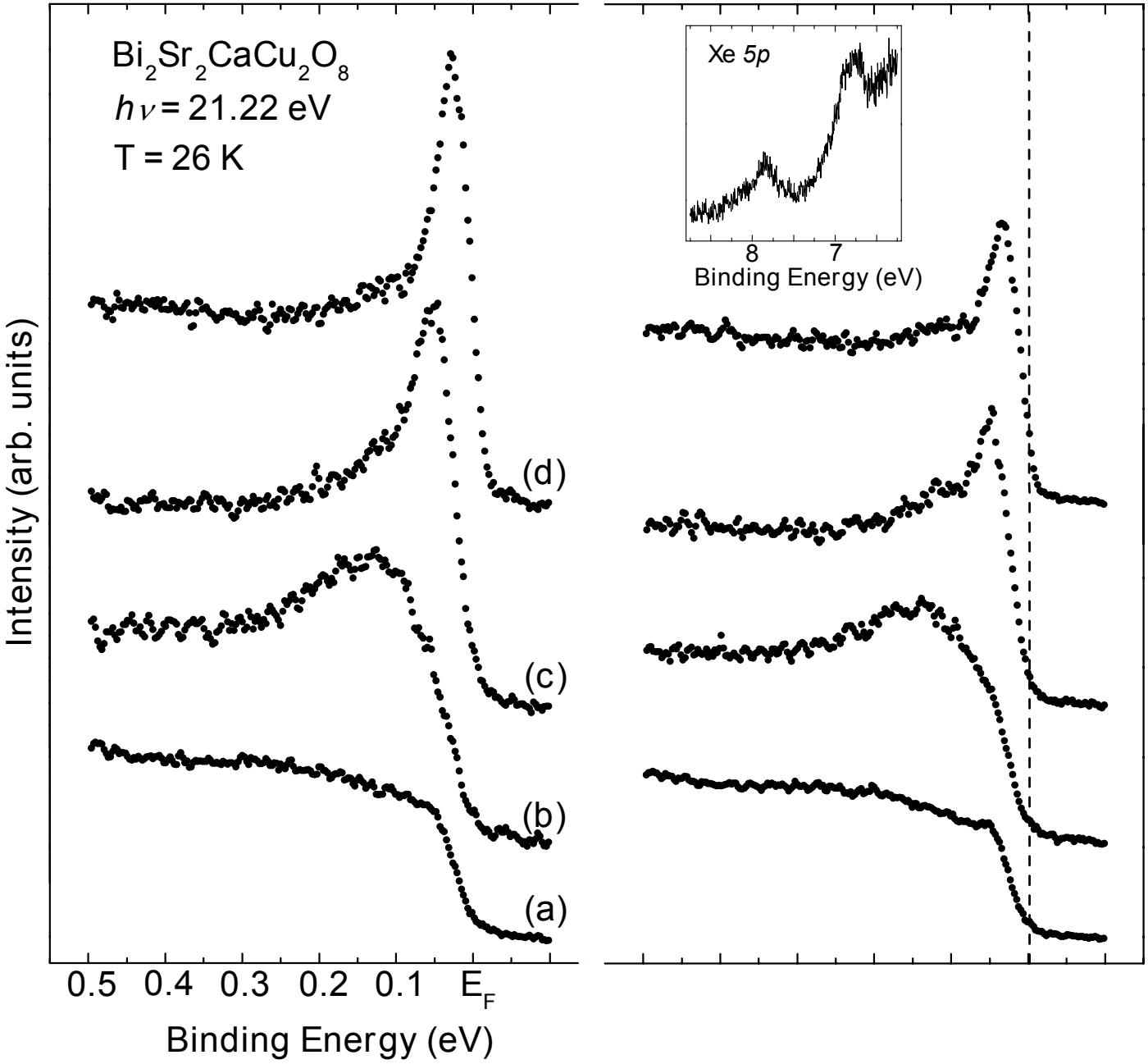
Bi2Sr2CaCu2O8
hν = 21.22 eV
T = 26 K
Intensity (arb. units)
(d)
(c)
(b)
(a)
0.5 0.4 0.3 0.2 0.1 EF
Binding Energy (eV)
Xe 5p
8 7
Binding Energy (eV)

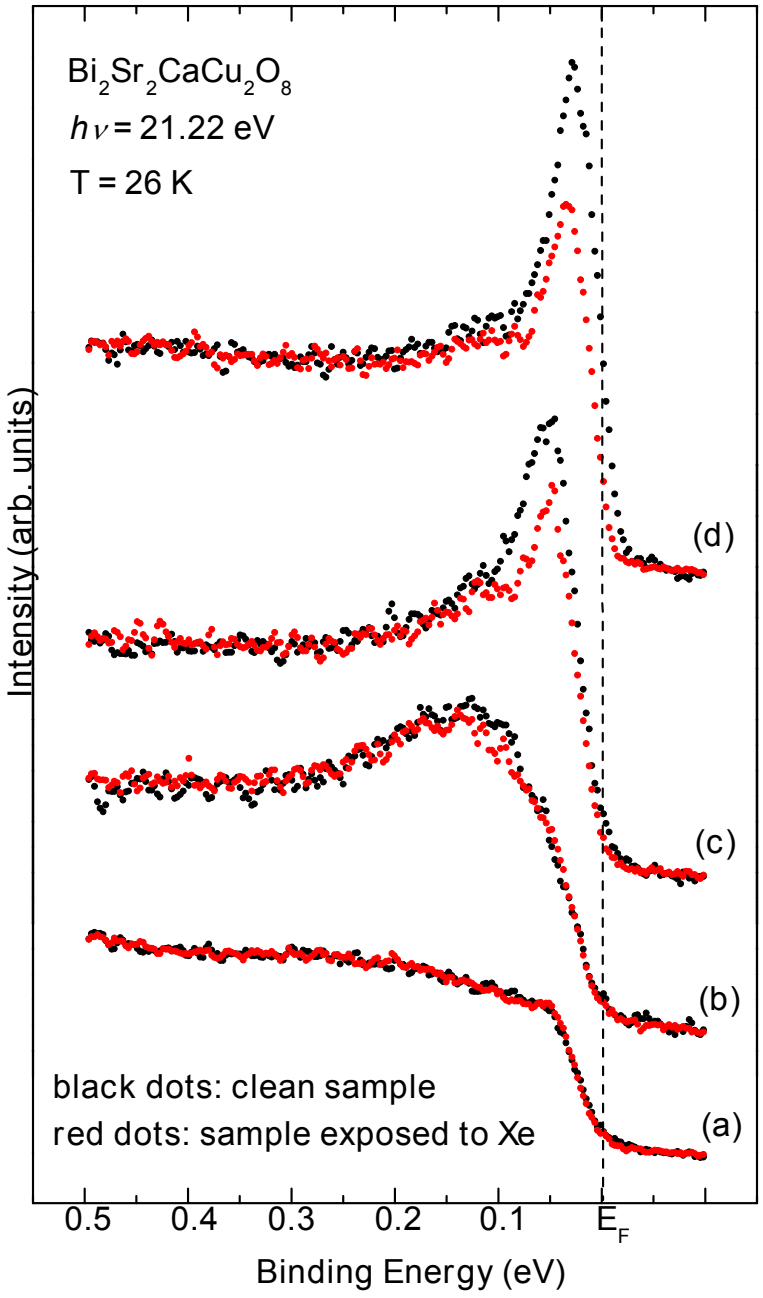
$Bi_2Sr_2CaCu_2O_8$
$h\nu$ = 21.22 eV
T = 26 K
Intensity (arb. units)
(d)
(c)
(b)
(a)
black dots: clean sample
red dots: sample exposed to Xe
0.5
0.4
0.3
0.2
0.1
E_F
Binding Energy (eV)

Changes are not really consistent with the broadening of the spectral function expected in a simple model of el.-phonon coupling

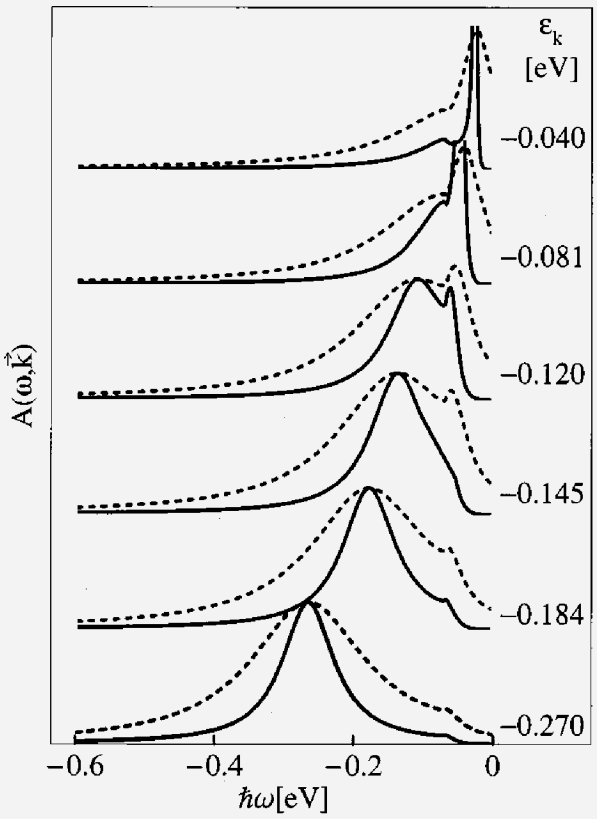

FIG. 1. Spectral function in the Debye model for $\omega_D = 65$ meV and $\lambda = 0.65$ with (dashed) and without (solid) a constant 54 meV added to Σ_I to represent impurity scattering.

S. LaShell, E. Jensen, and T. Balasubramanian, PRB 61, 2371 (2000)

Yet another unexpected result:
leading edge shifts by 7meV

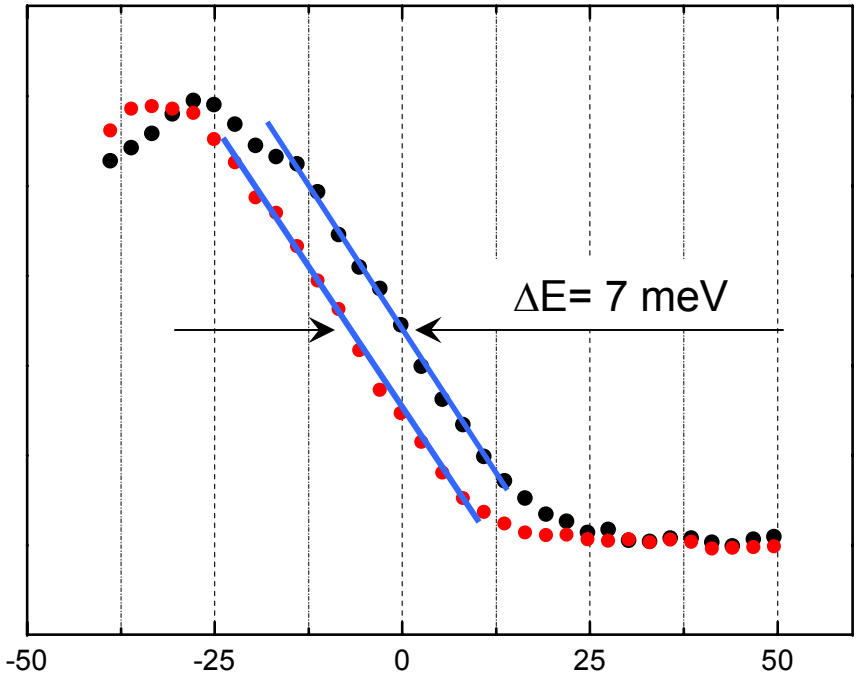

Spectra measured precisely at k_F

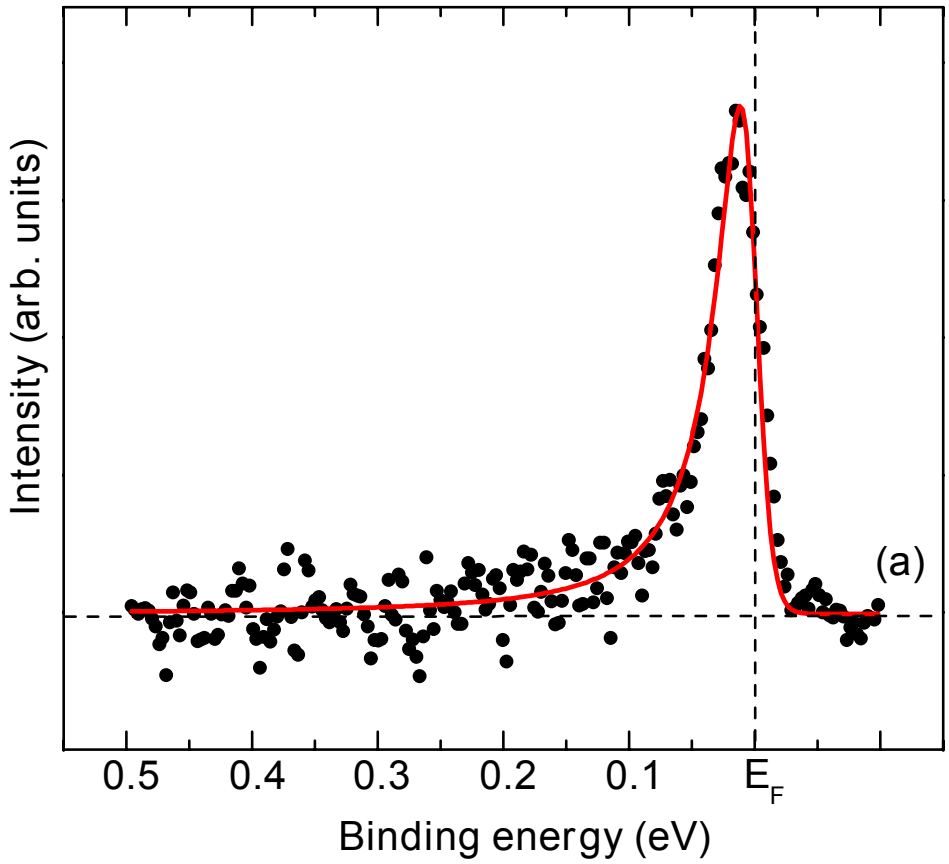

Red line is a fit to 50 meV wide Lorentzian exactly at the Fermi energy

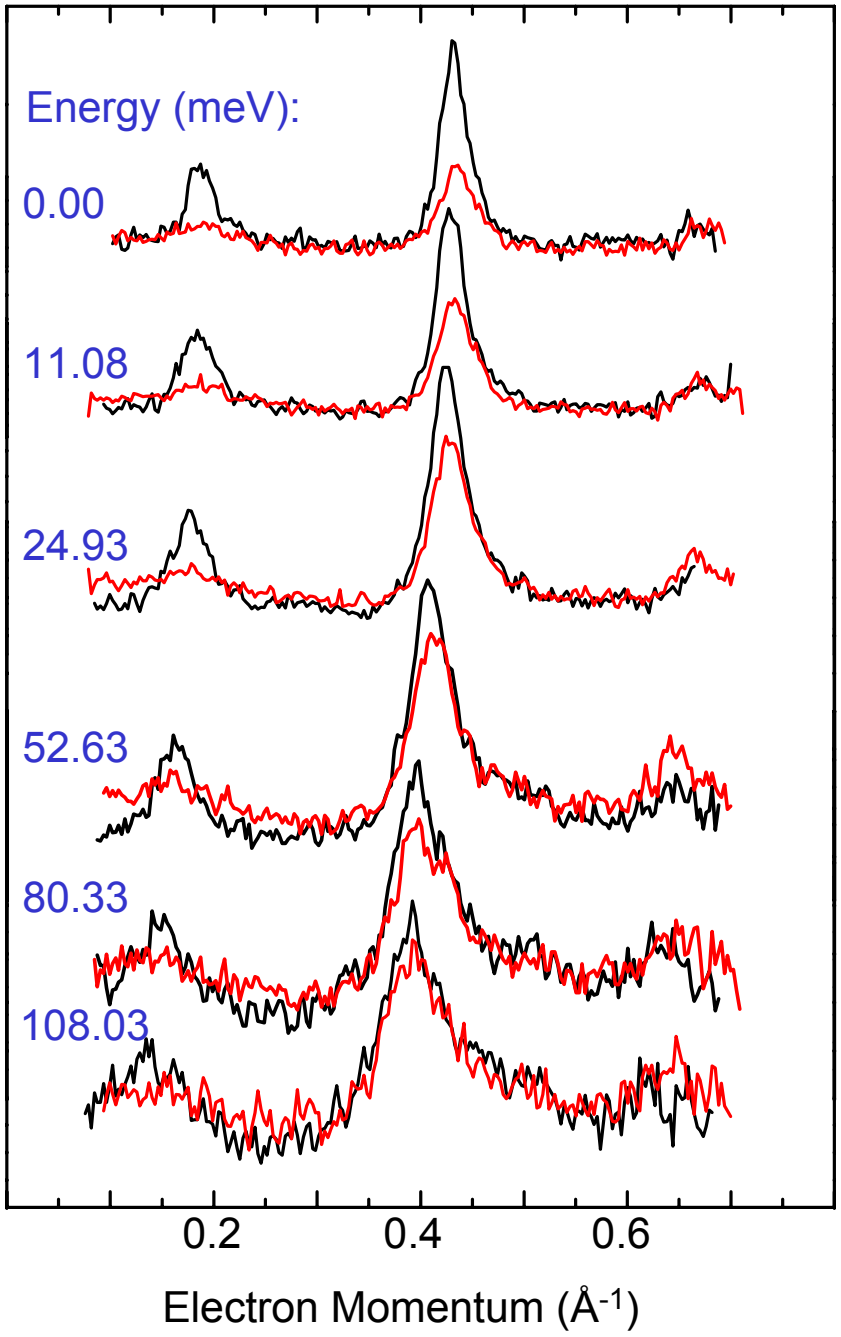
Energy (meV):
0.00
11.08
24.93
52.63
80.33
108.03
0.2
0.4
0.6
Electron Momentum (Å-1)

Making Good out of Evil

R.L. Withers et al.,
J. Phys. C 21, L417(1988)

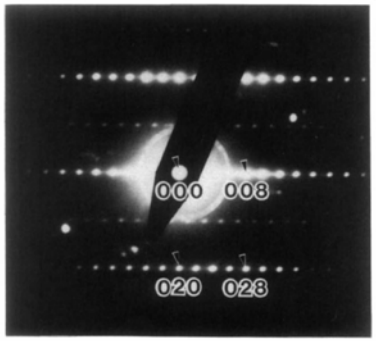

Figure 4. The [100] zone axis diffraction pattern of $Bi_2CaSr_2Cu_2O_x$ showing systematic extinction of reflections with $k + l \neq 2n$.

A. Yamamoto et al.,
PRB 42, 4228 (1990)

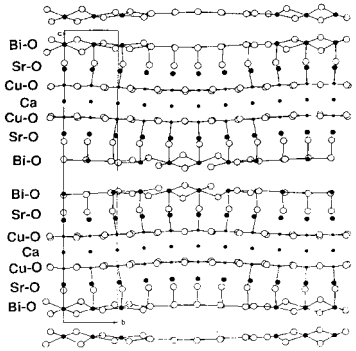

FIG. 6. The projection of the modulated structure of $Bi_2(Sr,Ca)_3Cu_2O_{8-\delta}$ along the *a* axis. Solid and open circles represent metal and oxygen atoms. The solid box is the outline of the unit cell. The five cells along the *b* direction are plotted, which correspond nearly to the one modulation period. The Cu—O bonds shorter than 2.5 Å and the Bi—O bonds shorter than 2.7 Å are plotted. The figure shows that some Cu—O bonds to the apical oxygens of the CuO_5 pyramid are longer than 2.5 Å.

Intensity of the umklapp band shows
non-monotonic behavior with energy

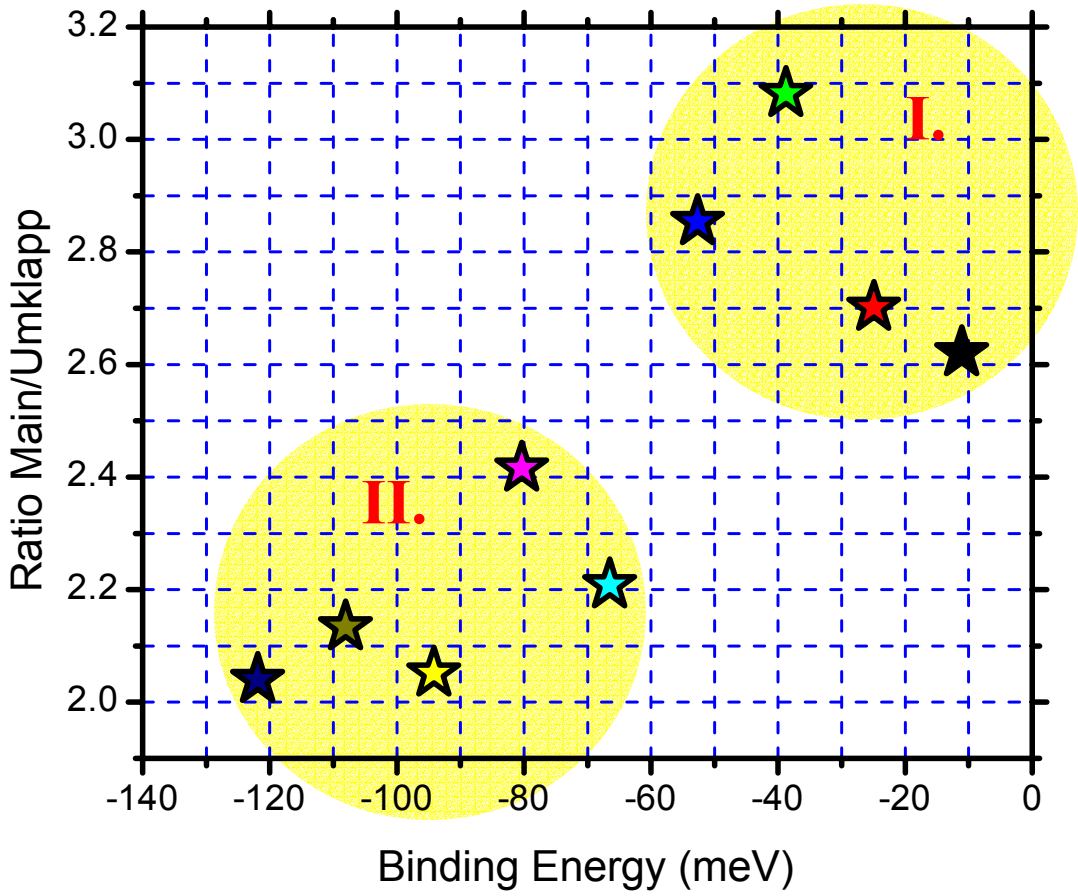

Zooming in the kinks

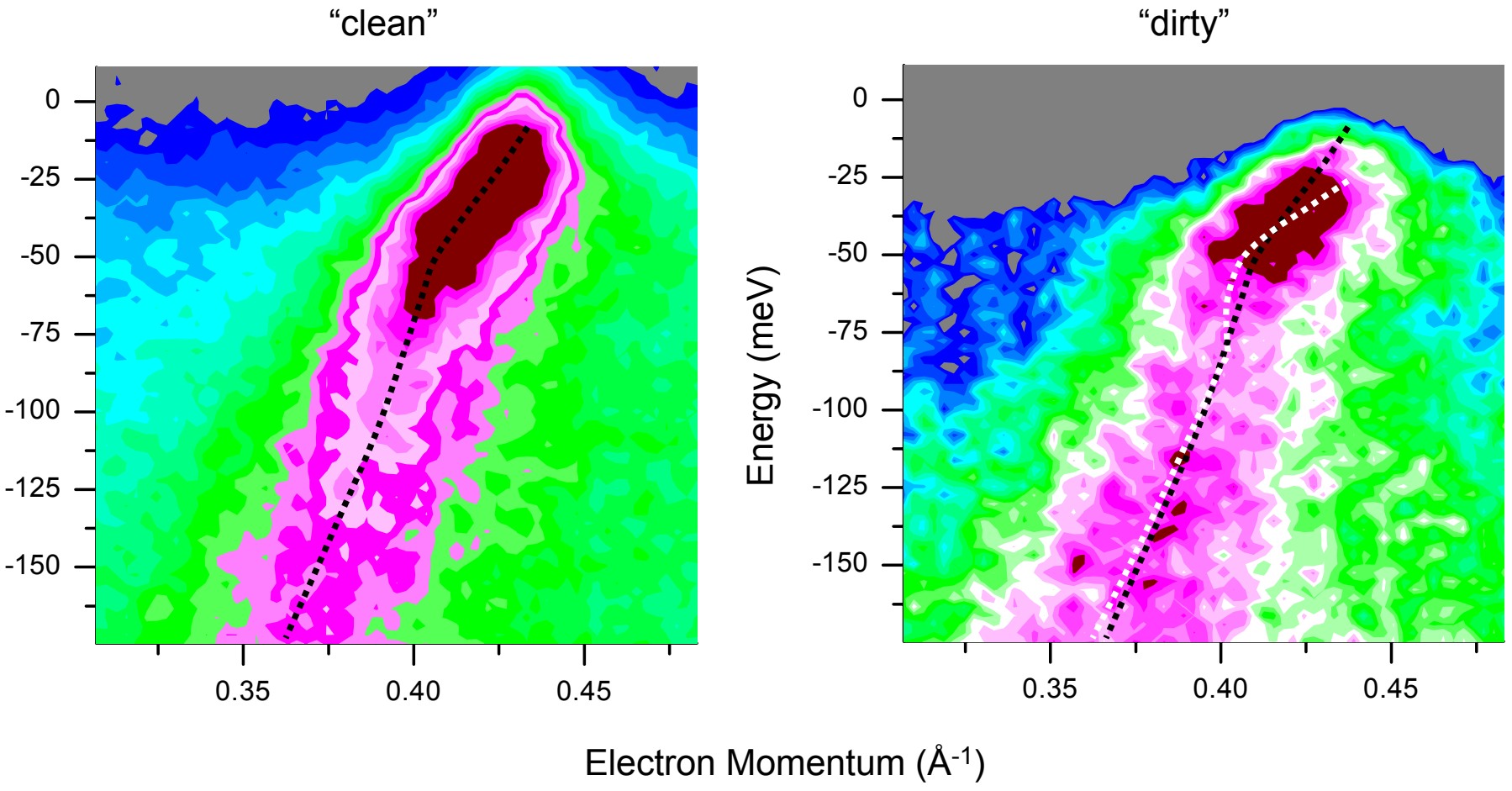

MDC Dispersions

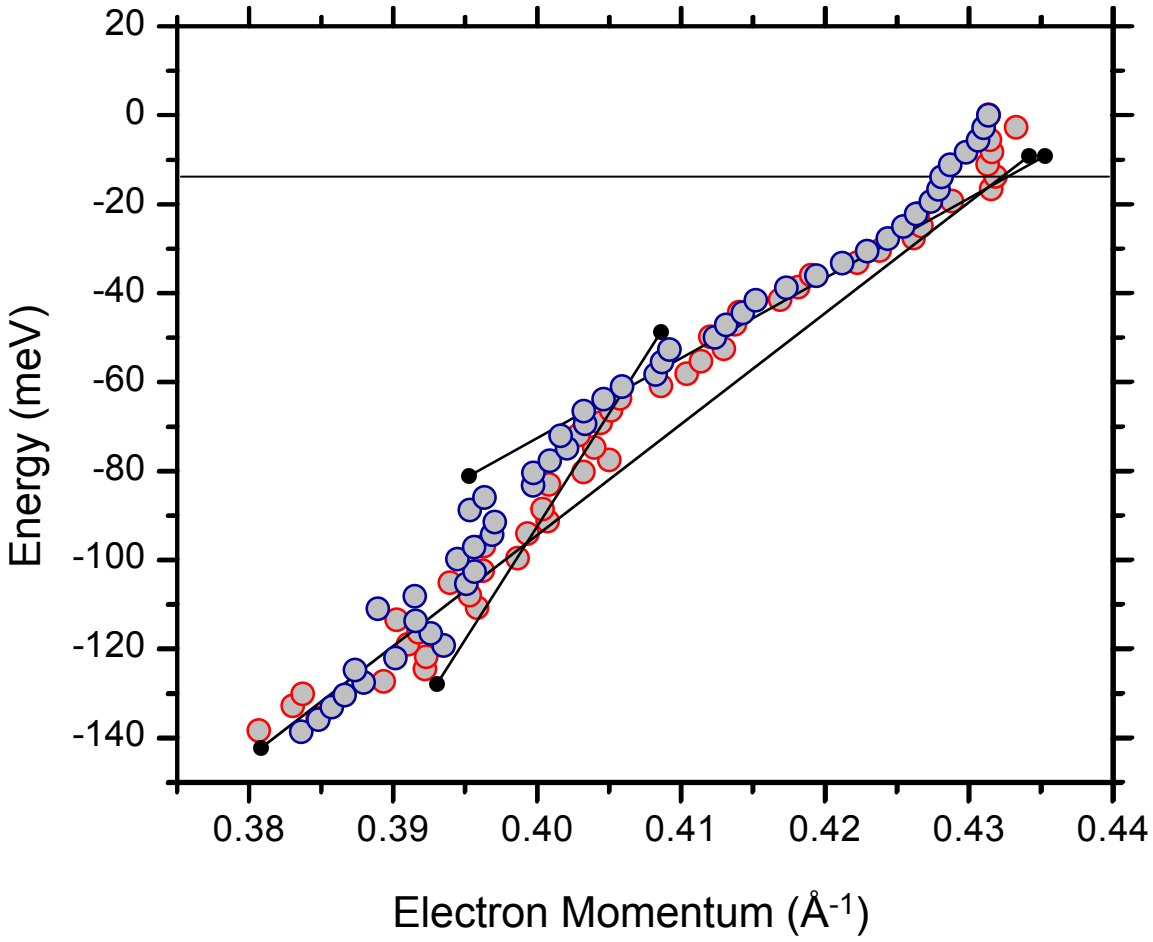

Implications & Speculations

Scenario A:
alignment along
Cu-Cu bond is OK

Scenario B:
it is not
OK

In any case we are dealing with the state which is sensitive to the surface conditions, i.e. a surface state

VOLUME 75, NUMBER 6 PHYSICAL REVIEW LETTERS 7 AUGUST 1995

Surface States and Angle-Resolved Photoemission Spectra from $Nd_{2-x}Ce_xCuO_4$ Superconductor

M. Lindroos[1,2] and A. Bansil[1]
[1]*Physics Department, Northeastern University, Boston, Massachusetts 02115*
[2]*Physics Department, Tampere University of Technology, Tampere, Finland*
(Received 3 February 1995)

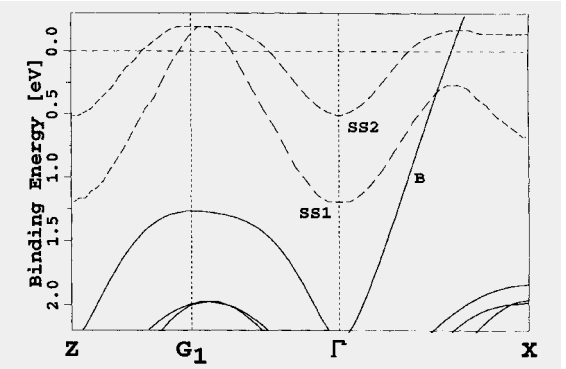

FIG. 4. Energy bands in the vicinity of E_F for the Γ-X and Γ-G_1-Z directions. Solid lines give the bulk bands, the dashed lines give the surface state bands related to SS1 and SS2.